

# **Scope of Work**

## **Project 22-019**

### **Refining ammonia emissions using inverse modeling and satellite observations over Texas and the Gulf of Mexico and investigating its effect on fine particulate matter**

Prepared for

The State of Texas Air Quality Research  
Program (AQRP)

By

University of Houston  
4800 Calhoun Road  
Houston, Texas 77204-5007

*Principal Investigator*

Yunsoo Choi

August 2022  
Version 1

QA Requirements: Audits of Data Quality: 10% Required  
Report of QA Findings: Required in Final Report

**NOTE: The Workplan package consists of three independent documents: Scope of Work, Quality Assurance Project Plan (QAPP), and budget and justification. Please deliver each document (as well as all subsequent documents submitted to AQRP) in Microsoft Word format.**

## **Approvals**

This Scope of Work was approved electronically on 09/01/2022 by Elena McDonald-Buller, The University of Texas at Austin

Elena McDonald-Buller

Project Manager, Texas Air Quality Research Program

This Scope of Work was approved electronically on 09/07/2022 by Khalid Al-Wali, Texas Commission on Environmental Quality

Khalid Al-Wali

Project Liaison, Texas Commission on Environmental Quality

## 1- Background

As ammonia ( $\text{NH}_3$ ) emissions exacerbate air quality and contribute to the formation of inorganic fine particulate matter ( $\text{PM}_{2.5}$ ), they are detrimental to human health by contributing to cardiovascular disease, asthma, and respiratory dysfunction (Pui et al., 2014; Cheng & Wang-Li, 2019). Owing to the contribution of  $\text{NH}_3$  concentrations to the formation of  $\text{PM}_{2.5}$  and its nonlinear relationship to the formation of ammonium nitrate (Zhu et al., 2015), the contribution of  $\text{NH}_3$  becomes even greater. It affects air quality and climate change by altering radiative forcing through aerosol formation (Hauglustaine et al., 2014), modifying the carbon flux (Pinder et al., 2013), modifying the phase of secondary inorganic aerosols (Yang et al., 2018), enhancing light absorption caused by organic aerosols (Huang et al., 2018), and heterogeneous ice nucleation (Kumar et al., 2018).  $\text{NH}_3$  also plays a major role in the nitrogen cycle by altering the nitrogen-containing compounds, including nitrous oxide ( $\text{N}_2\text{O}$ ) and nitrogen oxide ( $\text{NO}_x$ ) (Xu Zhenying et al., 2019). Excessive amounts of  $\text{NH}_3$  deposition can also harm sensitive ecosystems through soil acidification (Howard, 2011), loss of biodiversity (Carfrae et al., 2004), and eutrophication (Paerl et al., 2002). Although  $\text{NH}_3$  emissions significantly affect air quality, climate change, and public health, insufficient measurements have complicated the investigation of its effects (Momeni et al., 2022). Furthermore, the scarcity of related observations has resulted in significant uncertainties in modeling  $\text{NH}_3$  and designing regulatory control plans (Paulot et al., 2014). Scarcity of reliable information regarding the spatial and temporal distribution of emissions, emission factors, management practices, and farming plans (Zhu et al., 2013; Zhu et al., 2015) have also resulted in uncertainties in bottom-up  $\text{NH}_3$  emissions inventories.

Inverse modeling approaches using observational data are a well-known method of constraining modeling predictions and refining emissions inventories. Observational data often used for inverse modeling techniques are those obtained from remote sensing, such as ammonia ( $\text{NH}_3$ ) columns from the Cross-track Infrared Sounder (CrIS) instrument. Although remote sensing data have significantly contributed to our understanding of the spatial patterns of pollutant columns, they are often limited because of deficient spatial and temporal coverage and a significant level of uncertainty associated with measurements. As opposed to remote sensing data, chemical transport models (CTM) provide comprehensive data with a high spatiotemporal resolution of all species, our information from CTM, however, is also uncertain due to the numerical representation of chemical and physical processes in the atmosphere, as well as uncertainties in modeling inputs. As inverse modeling techniques help

leverage strengths in modeling data and observations, they improve modeling predictions by accounting for uncertainties in both predictions and observational data.

With this grant, Grantee will conduct an inverse modeling study over the state of Texas and the Gulf of Mexico using Community Multiscale Air Quality (CMAQ) models with the implementation of NH<sub>3</sub> remote sensing data from CrIS for 2019. Grantee will analyze NH<sub>3</sub> emissions from mobile, area, and point sources and emissions from anthropogenic and biogenic sources. In the inverse modeling study, Grantee will use satellite observations to update NH<sub>3</sub> emissions to constrain associated emissions, which are highly uncertain owing to a lack of NH<sub>3</sub> observations, resulting in errors in bottom-up calculated emissions. We will employ the iterative Finite Difference Mass Balance (iFDMB) inverse modeling technique to revise NH<sub>3</sub> emissions with respect to CrIS observations. Since running the iFDMB is computationally expensive and requires numerous iterations, using a reduced complexity CMAQ model (RCCM) for simulations will reduce the burden of computations while maintaining the accuracy of predictions. After updating the emissions inventory, Grantee will investigate the effect of adjusting NH<sub>3</sub> emissions on atmospheric chemistry, including PM<sub>2.5</sub> concentrations, and PM<sub>2.5</sub> inorganic and organic constituents.

## **2- Statement of Work**

### **2-1- Objectives of the Present Study**

Grantee shall produce a Draft and a Final Report detailing the following:

1. A detailed list of input files from other models and emissions inventories including meta-data describing their sources and parameterizations or configurations such as but not limited to:
  - a. U.S. EPA National Emissions inventory for 2017 (NEI2017) for emissions in Texas
  - b. The Cross-track Infrared Sounder (CrIS) satellite data for 2019
  - c. Sparse Matrix Operator Kernel Emissions (SMOKE) model for emission processing
  - d. Weather Research & Forecasting (WRF) model and Meteorology-Chemistry Interface Processor (MCIP) for meteorological simulations; and
  - e. Community Multi-scale Air Quality (CMAQ) model for air quality.

2. Documentation of pre-processing, installation, and testing of necessary modeling components;
3. Specifications of model configurations employed including details regarding the modeling domain, vertical layer structure, initial and boundary conditions, WRF physics options, ‘nudging’ methods and datasets applied, if any, chemical mechanism (e.g., CB05), method(s) of horizontal and vertical advection, method(s) of diffusion, and other major CMAQ configurations (e.g., lightning, chemistry, aerosols, clouds);
4. Validation and diagnostic methods employed for quality assurance of simulations using available in situ or remotely-sensed measurements. This will be performed in accordance with EPA guidelines regarding model evaluation.
5. Results of validation and diagnostic methods and error-checking including diagnostic plots and standard model performance statistics and visualizations including normalized mean bias (NMB), normalized mean error (NME), mean normalized bias (MNB), mean normalized error (MNE), root mean squared error (RMSE) and the coefficient of determination ( $r^2$ ); and
6. Characterization of model estimates obtained after updating emissions such as mean and maximum values at locations, measures of uncertainty, identification of instances of large relative differences between priori and posterior and other measures as appropriate.

## **2-2- Specific Implementation Tasks**

### **2-2-1- Preparation of model input files, comprehensive satellite, in situ, and modeling data for the iterative Finite Difference Mass Balance (iFDMB) method, perform photochemical modeling, and create an archive of results**

**(Dr. Yunsoo Choi and Ph.D. students, Mahmoudreza (Semko) Momeni, Arash Kashfi Yeganeh, Hadi Zanganeh Kia)**

Grantee or its designee shall acquire and appropriately modify input files required for meteorological and photochemical modeling using CMAQ and the inverse technique. Such input files include point, area, mobile and biogenic source emissions inventories and also  $\text{NH}_3$  satellite data. Simulation parameters are shown in Table 1.

Table 1: Simulation parameters

Simulation Parameter	Description	Comments
Simulation Episode	January 1-December 31, 2019	Excluding model “spin-up” period needed to account for boundary conditions
Simulation domain	State of Texas and Gulf of Mexico	
Resolution	12 km Texas	
Simulation runs	“a-priori” run (emissions or concentrations before updating) and “a-posteriori” run (emissions or concentrations after updating)	
Evaluation metrics	Normalized Mean Bias (NMB) Normalized Mean Error (NME) Mean Normalized Bias (MNB) Mean Normalized Error (MNE) Root Mean Squared Error (RMSE) Index of Agreement (IOA)	Used for both WRF and CMAQ

## 2-2-1-1- WRF runs

### i- Domain setup

The WRF domains have sizes of 132×126 for the 12-km domain covering Texas, as depicted in Figure 1.

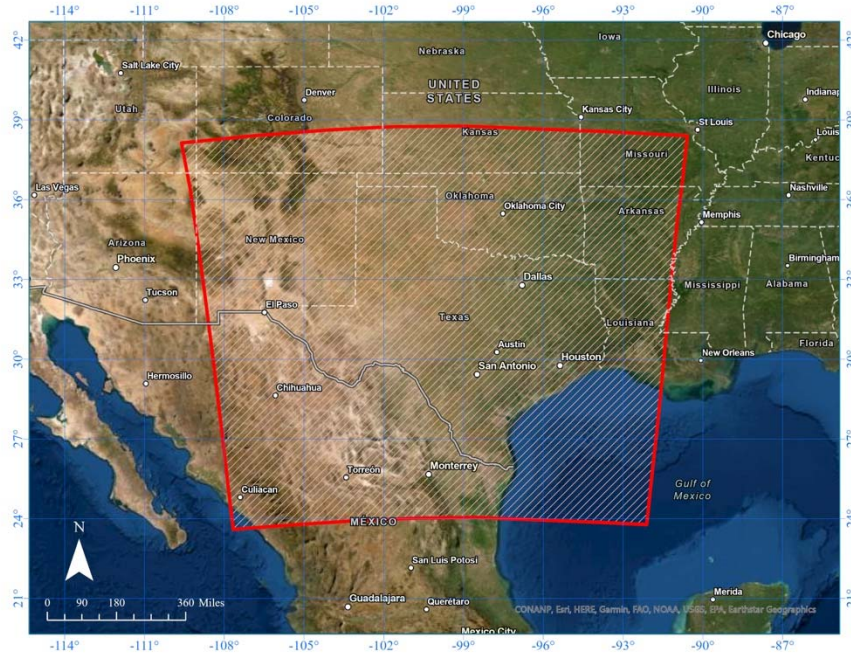


Figure 1: The modeling domain with WRF.

### ii- Input analysis data for WRF

We will use North American Mesoscale Forecast System (NAM) reanalysis datasets as input for running the WRF model. The NAM data (<https://rda.ucar.edu/datasets/ds609.0/>) has a horizontal

resolution of 12 km with a 6-hour temporal resolution. If there were missing data in NAM, we would use National Centers for Environmental Prediction (NCEP) North American Regional Reanalysis (NARR) data (<https://rda.ucar.edu/datasets/ds608.0/>) to fill the missing data.

### iii- Proposed major WRF configurations

Proposed WRF options are shown in Table 2 below. The first guess and boundary conditions will be generated by NAM reanalysis datasets.

Table 2: WRF model configurations for this study

WRF Version	V4.2 (V3.8*)
Microphysics	Lin et al. Scheme
Long-wave Radiation	Rapid Radiative Transfer Model for GCMs (RRTMG)
Short-wave Radiation	Rapid Radiative Transfer Model for GCMs (RRTMG)
Surface Layer Option	Pleim-Xu
Land-Surface Option	Unified Noah LSM (Land Surface Model)
Urban Physics	None
Boundary Layer Scheme	ACM2 (Pleim) scheme
Cumulus Cloud Option	Kain-Fritsch

\* If there were issues for the WRF 4.2 version due to updates on the supercomputer, WRF 3.8 version would be used.

## 2-2-1-2- CMAQ runs with the 2017 National Emissions inventory

### i- Emission processing

Emissions input for running the Chemical Transport Model (CTM) will be obtained from the National Emissions Inventory (NEI) (Eyth et al., 2022). EPA provides information on the emission of pollutants in the atmosphere through the National Emissions Inventory (NEI), which is a comprehensive and detailed estimate of air emissions of criteria pollutants, criteria precursors, and hazardous air pollutants from different air emissions sources such as NEI point sources, NEI nonpoint sources, NEI onroad sources, and NEI nonroad sources. We will use the NEI modeling platform that uses NEI emissions inventory and Sparse Matrix Operator Kernel Emissions (SMOKE) to spatially and temporally allocate the emission values to modeling grids. Emissions from natural sources will be estimated with Biogenic Emissions Inventory System (BEIS3). The mobile emissions will be processed based 2017 Motor Vehicle Emission Simulator (MOVES) output within the NEI package. NEI modeling platform 2017 will be used to produce emissions at 12km spatial resolution for Texas for the whole year of 2019.

## ii- Generating meteorological input using MCIP

Meteorological input for CMAQ will be processed using MCIP over the WRF output.

## iii- Proposed major CMAQ configurations

Proposed major CMAQ configurations are shown in Table 3.

Table 3: CMAQ model configurations for this study.

CMAQ version	V5.0.1, the latest is v5.3.2
Domain size	121×115
Chemical Mechanism	cb05tucl_ae5_aq: Carbon-Bond version 5 (CB05) gas-phase mechanism with active chlorine chemistry, updated toluene mechanism, fifth-generation CMAQ aerosol mechanism with sea salt, aqueous/cloud chemistry
Lightning NOx emissions	Included by using inline code
Horizontal advection	Yamartino Scheme
Vertical advection	WRF omega formula
Horizontal mixing/diffusion	Multiscale
Vertical mixing/diffusion	Asymmetric Convective Model version 2
Chemistry solver	Euler Backward Iterative (EBI) optimized for the Carbon Bond-05 mechanism
Aerosol physics and chemistry	Aerosol module version 5 (AERO5) for sea salt and thermodynamics
Cloud Option	Asymmetric Convective Model (ACM)
Initial Condition (IC) / Boundary Condition (BC)	Default static profiles

## 2-2-1-3- Preparation of comprehensive satellite and in situ observations

### i- Cross-track Infrared Sounder (CrIS)

In this project, we will use the Cross-track Infrared Sounder (CRIS) satellite observations for NH<sub>3</sub>. The CrIS instrument is an infrared sounder onboard the sun-synchronous satellite Suomi National Polar-orbiting Partnership (SNPP) (Shephard & Cady-Pereira, 2015) mission, launched in October 2011, with a mean local daytime overpass time of 13:30 and a mean local nighttime overpass time of 01:30. CrIS provides an across-track scanning swath width of 2,200 km and a nadir spatial resolution of 14 km (Dammers et al., 2017). For the preparation of the CrIS satellite observations for this project, we will employ a CrIS observation operator developed by Momeni et al. (2022). In the next sections, the CrIS observation operator is explained.

## ii- In-Situ observations

To evaluate the output of models (WRF and CMAQ) and also, the inverse method, we use NCEP Meteorological Assimilation Data Ingest System (MADIS) (<https://madis.noaa.gov/>) for meteorological parameters, surface measurements from the AMoN (<http://nadp.sws.uiuc.edu/AMoN/>) for NH<sub>3</sub> concentrations, the South Eastern Aerosol Research and Characterization Network (SEARCH) networks, and ammonium (NH<sub>4</sub><sup>+</sup>) wet deposition measurements from the National Atmospheric Deposition Program (NADP) network (<http://nadp.slh.wisc.edu/ntn/>). Additionally, remote-sensing data from the CrIS satellites will also be employed.

## 2-2-2- Preparation of the iterative Finite Difference Mass Balance (iFDMB) to refine ammonia emissions

(Dr. Yunsoo Choi and Ph.D. students, Mahmoudreza (Semko) Momeni, Arash Kashfi Yeganeh, Hadi Zanganeh Kia)

### 2-2-2-1- iterative Finite Difference Mass Balance (iFDMB)

In this project, we will apply the iFDMB inverse modeling to refine the NH<sub>3</sub> emissions inventories implemented by Momeni et al. 2022. In the iFDMB, a-priori concentrations retrieved using a forward model will be used to linearize the sensitivity of the column density ( $\Omega$ ) to NH<sub>3</sub> emissions ( $E$ ) at every grid point. Then, top-down emissions ( $E_t$ ) are calculated at each iteration as follows:

$$E_t = E_a \left(1 + \frac{1}{\beta} \frac{\Omega_o - \Omega_a}{\Omega_a}\right), \quad (1)$$

where  $E_a$  presents a-priori emissions from the previous iteration,  $\Omega_o$  the observed column,  $\Omega_a$  the simulated column, and  $\beta$  the initial sensitivity given as:

$$\beta = \frac{\Delta\Omega/\Omega}{\Delta E/E}. \quad (2)$$

A perturbation of 20% to the a-priori emissions,  $E$ , is applied in each grid to determine the initial sensitivity. The iteration process is repeated until the normalized mean error (NME) of new emissions with respect to the emissions calculated from the last iteration is less than 1% or 2%. In Figure 2, a schematic diagram of iFDMB is shown.

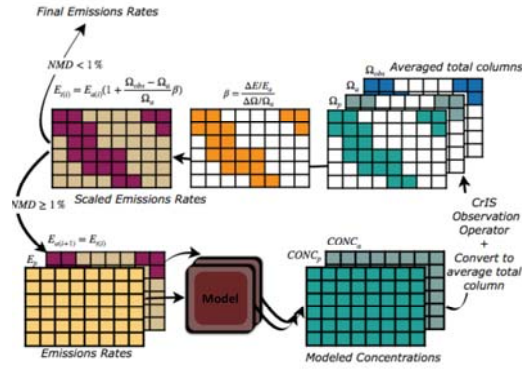


Figure 2: Schematic diagram of how iFDMB works (source: Chen et al., Atmos. Chem. Phys. Discuss., 2020).

### 2-2-2-2- Reduced-Complexity CMAQ Model (RCCM) for NH<sub>3</sub>

The iFDMB technique performs multiple model simulations to be converged to the final results. To reduce the computational cost, a Reduced-Complexity CMAQ Model (RCCM) will be employed to simulate NH<sub>3</sub>. In the RCCM, NH<sub>3</sub> and NH<sub>4</sub><sup>+</sup> are considered as two tracer pollutants of the model, and all of the chemical processes of other species are turned off. The developed RCCM included dry and wet deposition, the transport of NH<sub>3</sub> and NH<sub>4</sub><sup>+</sup>, and NH<sub>x</sub> partitioning; the subroutine of ISORROPIA-II in the aerosol module calculates the gas-particle partitioning of NH<sub>3</sub> and NH<sub>4</sub><sup>+</sup>. In this project, we will evaluate the RCCM over Texas using the comparison between the concentration of NH<sub>3</sub>, NH<sub>4</sub><sup>+</sup>, sulfate (SO<sub>4</sub><sup>2-</sup>), and nitrate (NO<sub>3</sub><sup>-</sup>) simulated by the RCCM and those by the full model to make sure that the RCCM model produces reasonable results.

### 2-2-2-3- CrIS Observation Operator

In order to employ the iFDMB technique to improve NH<sub>3</sub> emissions, satellite data from the CRIS satellite observations will be used for this project. For operating the iFDMB, only valid pixels with quality flag values exceeding 3 will be selected.

To apply the iFDMB inverse modeling and to also compare model estimates to satellite observations, we will use the vertical column of the model by summing a modeled partial column from Herron-Thorpe et al. (2010), which is in molecule cm<sup>-2</sup>, as follows:

$$VCD_i = \frac{c_i}{10^6} \times \frac{L_{T_i} \times P_i \times N_A}{R \times T_i}, \quad (3)$$

where the *i* index is the level number, *c* the concentration of NH<sub>3</sub> in ppmv, *L<sub>T<sub>i</sub></sub>* the model layer thickness, *P* the pressure in pascals, *N<sub>A</sub>* avogadro's number, *R* the molar gas constant, and *T* the

temperature in Kelvins. By substituting the equation of state and the hydrostatic equation into Equation (3), the vertical column density can be given by

$$VCD_i = -c_i \times \Delta P_i \times 2.119 \times 10^{14}. \quad (4)$$

For CrIS, since the averaging kernel is provided, we will calculate the column density by using the observational operator,  $H$ , to estimate the model  $\text{NH}_3$  profile:

$$Hc = c_a + A(Mc - c_a), \quad (5)$$

where  $c$  is the model-estimated  $\text{NH}_3$  profile,  $M$  a matrix that maps the space of the model to the space of CrIS,  $A$  the averaging kernel, and  $c_a$  the a-priori  $\text{NH}_3$  profile (Shephard et al., 2011). The total vertical column density of the model is calculated as

$$VCD = \sum_i VCD_i. \quad (6)$$

### **2-2-3- Top-down estimation of $\text{NH}_3$ emissions inventory and the evaluation of updated emissions inventory**

**(Dr. Yunsoo Choi and Ph.D. students, Mahmoudreza (Semko) Momeni, Arash Kashfi Yeganeh, Hadi Zanganeh Kia)**

We will adjust  $\text{NH}_3$  emissions using the CrIS  $\text{NH}_3$  column retrievals by the iFDMB. Following this method, we will develop adjusting factors to modify  $\text{NH}_3$  emissions until they reach an optimum state in which  $\text{NH}_3$  concentrations are close to the CrIS observations (shown in Figure 2). In this project, our domain covers the whole of Texas and some part of the Gulf of Mexico and the  $\text{NH}_3$  emissions will be updated over these regions. After adjusting the emissions, the CMAQ model will be run with the configurations and inputs listed and described in the previous sections, with a-priori emissions (emissions before updating) and a-posteriori emissions (updated emissions) in 2019. Model-measurement comparisons will be made for ammonia and inorganic fine particulate matter, and the model evaluations will be made as per the metrics listed in Table 3. We will evaluate adjusted emissions by the comparison of in-situ and satellite observations with concentrations modeled by a-priori emissions and a-posteriori emissions. To address this uncertainty, we will first compare  $\text{NH}_3$ ,  $\text{NH}_4^+$ ,  $\text{SO}_4^{2-}$ , and  $\text{NO}_3^-$  species modeled using the a-posteriori and a-priori emissions with those measured by surface stations (if available) and then we will analyze the spatial distribution of the species. Over Texas (land), we will use both satellite and in-situ observations to evaluate a-posteriori and a-priori emissions and to also find the uncertainty in  $\text{NH}_3$  emissions. To address this uncertainty, we will compare the  $\text{NH}_3$ ,  $\text{NH}_4^+$ ,  $\text{SO}_4^{2-}$ , and  $\text{NO}_3^-$  species modeled using the a-posteriori and a-priori emissions with those measured by surface stations and then we will analyze the spatial

distribution of the species. Over the Gulf of Mexico, we consider only  $\text{NH}_3$  species and we will compare the  $\text{NH}_3$  vertical column density modeled using the a-posteriori and a-priori emissions with those obtained from CrIS satellite observations. In the final, we will analyze the spatial distribution of the species over Texas and the Gulf of Mexico.

#### **2-2-4- Investigation of $\text{PM}_{2.5}$ concentrations using updated emissions inventory**

**(Dr. Yunsoo Choi and Ph.D. students, Mahmoudreza (Semko) Momeni, Arash Kashfi Yeganeh, Hadi Zanganeh Kia)**

We will explore changes in  $\text{PM}_{2.5}$  concentrations after adjusting the  $\text{NH}_3$  emissions inventory and calculating the contribution of inorganic  $\text{PM}_{2.5}$  in total  $\text{PM}_{2.5}$ . In inorganic  $\text{PM}_{2.5}$ ,  $\text{NH}_3$  tends to neutralize  $\text{SO}_4^{-2}$  first and then reacts with  $\text{NO}_3^-$  if free  $\text{NH}_3$  exists, and when the regime is ammonia-poor, ammonium nitrate will be low or close to zero; otherwise, when  $\text{SO}_4^{-2}$  is not present to be neutralized by  $\text{NH}_3$ , the  $\text{NH}_3$  reacts with  $\text{NO}_3^-$  (Seinfeld & Pandis, 2016). We will investigate changes in the chemistry of particles resulting from changes in  $\text{NH}_3$  emissions. We will show the contribution of updated  $\text{NH}_3$  emissions in  $\text{PM}_{2.5}$ .

#### **2-2-5- Comparison between model output using a-priori emissions and those using a-posteriori emissions to quantify the magnitude of ammonia over Texas and the Gulf of Mexico**

**(Dr. Yunsoo Choi and Ph.D. students, Mahmoudreza (Semko) Momeni, Arash Kashfi Yeganeh, Hadi Zanganeh Kia)**

As indicated in the previous sections, the CMAQ model will be run with the configurations and inputs listed and described in the previous sections, with a priori emissions in 2019. Model-measurement comparisons for a-priori and a-posteriori cases will be made for ammonia and fine particulate matter, and the model evaluations will be made as per the metrics listed in Table 3. The model performed using a-priori and a-posteriori emissions will be evaluated against in-situ measurements from several sources, such as surface measurements from the Ammonia Monitoring Network (AMoN) (<http://nadp.sws.uiuc.edu/AMoN/>) and the SouthEastern Aerosol Research and Characterization Network (SEARCH) networks, and  $\text{NH}_4^+$  wet deposition measurements from the NADP network (<http://nadp.slh.wisc.edu/ntn/>). Additionally, remote-sensing data from the CrIS satellites will also be employed.

### 3- Work Schedule

Task	Sep 2022	Oct 2022	Nov 2022	Dec 2022	Jan 2023	Feb 2023	Mar 2023	Apr 2023	May 2023	Jun 2023	July 2023	Aug 2023
Preparing met data	■											
Running met model (WRF)	■	■										
Evaluating met model result			■									
Preparing emission data		■										
Running emission model (SMOKE)		■	■									
Preparing satellite and in-situ data	■	■	■	■								
Running framework (iFDMB)				■	■	■						
Running standard CMAQ with a-priori and a-posteriori emissions							■	■	■			
Evaluating a-priori and a-posteriori NH <sub>3</sub> concentrations									■	■		
Evaluating a-priori and a-posteriori NH <sub>3</sub> concentrations										■	■	
Investigating PM <sub>2.5</sub> concentrations using updated emissions											■	
Comparing model output using a-priori emissions with those using a-posteriori emissions										■	■	
Technical Reports	■	■	■	■	■	■	■	■	■	■		
Financial Reports	■	■	■	■	■	■	■	■	■	■	■	■
Quarterly Reports		■			■			■			■	
Draft Final Report											■	
Final Report												■
AQRP Workshop												■

### 4- Deliverables

A set of electronic files containing input files (a priori emissions, meteorology, configurations), the output of iFDMB framework (a posteriori inventories and convergence files), and output results of CMAQ modeling under a priori and a posteriori emissions inventories and dates requested following the specified protocols.

The expected deliverable date: **September 20, 2023**

### 5- Reporting

As required, monthly technical, monthly financial status, and quarterly reports as well as an abstract at project initiation and, near the end of the project, the draft final and final reports will be submitted according to the schedule below. Dr. Choi or his designee will electronically submit each

report to both the AQRP project manager and the TCEQ liaisons and will follow the State of Texas accessibility requirements as set forth by the Texas State Department of Information Resources (<http://aqrp.ceer.utexas.edu/>). A representative from the project will present at the AQRP Workshop. Draft copies of any planned presentations (such as at technical conferences) or manuscripts to be submitted for publication resulting from this project will be provided to both the AQRP and TCEQ liaisons per the Publication/Publicity Guidelines included in Attachment G of the subaward. Final project data and associated metadata will be prepared and submitted to the AQRP archive. Each deliverable and required deadline for submission are presented below.

### **5-1- Abstract**

At the beginning of the project, an Abstract will be submitted to the Project Manager for use on the AQRP website. The Abstract will provide a brief description of the planned project activities and will be written for a non-technical audience.

Abstract Due Date: **September 1, 2022**

### **5-2- Quarterly Reports**

Each Quarterly Report will provide a summary of the project status for each reporting period. It will be submitted to the Project Manager as a Microsoft Word file. It will not exceed 2 pages and will be text only. No cover page is required. This document will be inserted into an AQRP compiled report to the TCEQ.

Quarterly Report Due Dates:

Report	Period Covered	Due Date
Quarterly Report #1	September-October 2022	October 31, 2022
Quarterly Report #2	November 2022-January 2023	January 31, 2023
Quarterly Report #3	February-April 2023	April 30, 2023
Quarterly Report #4	May-July 2023	July 31, 2023

### **5-3- Monthly Technical Reports (MTRs)**

Technical Reports will be submitted monthly to the Project Manager and TCEQ Liaison in Microsoft Word format using the AQRP Template found on the AQRP website

MTR Due Dates:

Report	Period Covered	Due Date
Technical Report #1	September 1-30, 2022	October 10, 2022
Technical Report #2	October 1-31, 2022	November 10, 2022
Technical Report #3	November 1-30, 2022	December 10, 2022
Technical Report #4	December 1-31, 2022	January 15, 2023
Technical Report #5	January 1-31, 2023	February 10, 2023
Technical Report #6	February 1-28, 2023	March 10, 2023
Technical Report #7	March 1-31, 2023	April 10, 2023
Technical Report #8	April 1-30, 2023	May 10, 2023
Technical Report #9	May 1-31, 2023	June 10, 2023
Technical Report #10	June 1-30, 2023	July 10, 2023

**5-4- Financial Status Reports (FSRs)**

Financial Status Reports will be submitted monthly to the AQRP Grant Manager (RoseAnna Goewey) by each institution on the project using the FSR Template found on the AQRP website.

FSR Due Dates:

Report	Period Covered	Due Date
Financial Report #1	September 1-30, 2022	October 10, 2022
Financial Report #2	October 1-31, 2022	November 10, 2022
Financial Report #3	November 1-30, 2022	December 10, 2022
Financial Report #4	December 1-31, 2022	January 15, 2023
Financial Report #5	January 1-31, 2023	February 10, 2023
Financial Report #6	February 1-28, 2023	March 10, 2023
Financial Report #7	March 1-31, 2023	April 10, 2023
Financial Report #8	April 1-30, 2023	May 10, 2023
Financial Report #9	May 1-31, 2023	June 10, 2023
Financial Report #10	June 1-30, 2023	July 10, 2023
Financial Report #11	July 1-31, 2023	August 10, 2023
Financial Report #12	August 1-31, 2023	August 31, 2023

**5-5- Draft Final Report**

A Draft Final Report will be submitted to the Project Manager and the TCEQ Liaison. It will include an Executive Summary. It will be written in third person and will follow the State of Texas accessibility requirements as set forth by the Texas State Department of Information Resources. It will also include a report of the QA findings.

Draft Final Report Due Date: **July 31, 2023**

## **5-6- Final Report**

A Final Report incorporating comments from the AQRP and TCEQ review of the Draft Final Report will be submitted to the Project Manager and the TCEQ Liaison. It will be written in third person and will follow the State of Texas accessibility requirements as set forth by the Texas State Department of Information Resources.

Final Report Due Date: **August 31, 2023**

## **5-7- Project Data**

All project data including but not limited to QA/QC measurement data, metadata, databases, modeling inputs and outputs, etc., will be submitted to the AQRP Project Manager within 30 days of project completion August 31, 2023. The data will be submitted in a format that will allow AQRP or TCEQ or other outside parties to utilize the information. It will also include a report of the QA findings.

AQRP Workshop: A representative from the project will present at the AQRP Workshop in the **August 15, 2022**.

## 6- References

- Carfrae, J. A., Sheppard, L. J., Raven, J. A., Leith, I. D., Stein, W., Crossley, A., & Theobald, M. (2004). Early effects of atmospheric ammonia deposition on *Calluna vulgaris* (L.) hull growing on an ombrotrophic peat bog. *Water, Air, and Soil Pollution: Focus*, 4(6), 229–239. <https://doi.org/10.1007/s11267-004-3033-1>
- Chen, Y., Shen, H., Kaiser, J., Hu, Y., Capps, S. L., Zhao, S., Hakami, A., Shih, J. S., Pavur, G. K., Turner, M. D., Henze, D. K., Resler, J., Nenes, A., Napelenok, S. L., Bash, J. O., Fahey, K. M., Carmichael, G. R., Chai, T., Clarisse, L., ... Russell, A. G. (2021). High-resolution hybrid inversion of IASI ammonia columns to constrain US ammonia emissions using the CMAQ adjoint model. *Atmospheric Chemistry and Physics*, 21(3), 2067–2082. <https://doi.org/10.5194/ACP-21-2067-2021>
- Cheng, B., & Wang-Li, L. (2019). Responses of secondary inorganic PM<sub>2.5</sub> to precursor gases in an Ammonia Abundant area in North Carolina. *Aerosol and Air Quality Research*, 19(5), 1126–1138. <https://doi.org/10.4209/aaqr.2018.10.0384>
- Dammers, E., Shephard, M. W., Palm, M., Cady-Pereira, K., Capps, S., Lutsch, E., Strong, K., Hannigan, J. W., Ortega, I., Toon, G. C., Stremme, W., Grutter, M., Jones, N., Smale, D., Siemons, J., Hrpcek, K., Tremblay, D., Schaap, M., Notholt, J., & Erisman, J. W. (2017). Validation of the CrIS fast physical NH<sub>3</sub> retrieval with ground-based FTIR. *Atmos. Meas. Tech.*, 10(7), 2645–2667. <https://doi.org/10.5194/amt-10-2645-2017>
- Eyth, A., Vukovich, J., Farkas, C., & Godfrey, J. (2022). Technical Support Document (TSD): Preparation of Emissions Inventories for the 2017 North American Emissions Modeling Platform. *U.S. Environmental Protection Agency Office of Air Quality Planning and Standards*. [https://www.epa.gov/system/files/documents/2022-03/2017\\_emismod\\_tsd\\_february2022\\_0.pdf](https://www.epa.gov/system/files/documents/2022-03/2017_emismod_tsd_february2022_0.pdf)
- Hauglustaine, D. A., Balkanski, Y., & Schulz, M. (2014). A global model simulation of present and future nitrate aerosols and their direct radiative forcing of climate. *Atmospheric Chemistry and Physics*, 14(20), 11031–11063. <https://doi.org/10.5194/acp-14-11031-2014>
- Herron-Thorpe, F. L., Lamb, B. K., Mount, G. H., & Vaughan, J. K. (2010). Evaluation of a regional air quality forecast model for tropospheric NO<sub>2</sub> columns using the OMI/Aura satellite tropospheric NO<sub>2</sub> product. *Atmospheric Chemistry and Physics*, 10(18), 8839–8854. <https://doi.org/10.5194/ACP-10-8839-2010>

- Howard, C. M. (2011). The European Nitrogen Assessment. The European Nitrogen Assessment, January. <https://doi.org/10.1017/cbo9780511976988>
- Huang, M., Xu, J., Cai, S., Liu, X., Zhao, W., Hu, C., Gu, X., Fang, L., & Zhang, W. (2018). Characterization of brown carbon constituents of benzene secondary organic aerosol aged with ammonia. *Journal of Atmospheric Chemistry*, 75(2), 205–218. <https://doi.org/10.1007/s10874-017-9372-x>
- Kumar, A., Marcolli, C., Luo, B., & Peter, T. (2018). Enhanced ice nucleation efficiency of microcline immersed in dilute  $\text{NH}_3$  and  $\text{NH}_4^+$ -containing solutions. *Atmospheric Chemistry and Physics Discussions*, January, 1–32. <https://doi.org/10.5194/acp-2018-46>
- Momeni, M., Choi, Y., Pouyaei, A., Kashfi Yeganeh, A., Jung, J., Park, J., Shephard, M. W., Dammers, E., Cady-Pereira, K. E. (2022). Application of iterative Finite Difference Mass Balance (iFDMB) Technique to Constrain East Asia Ammonia Emissions through Satellite Observations. *under revision*.
- Paerl, H. W., Dennis, R. L., & Whitall, D. R. (2002). Atmospheric deposition of nitrogen: Implications for nutrient over-enrichment of coastal waters. *Estuaries*, 25(4), 677–693. <https://doi.org/10.1007/BF02804899>
- Paulot, F., Jacob, D. J., Pinder, R. W., Bash, J. O., Travis, K., & Henze, D. K. (2014). Ammonia emissions in the United States, European Union, and China derived by high-resolution inversion of ammonium wet deposition data: Interpretation with a new agricultural emissions inventory (MASAGE\_NH3). *Journal of Geophysical Research: Atmospheres*, 119(7), 4343–4364. <https://doi.org/10.1002/2013JD021130>
- [Pinder, R. W., Bettez, N. D., Bonan, G. B., Greaver, T. L., Wieder, W. R., Schlesinger, W. H., & Davidson, E. A. \(2013\). Impacts of human alteration of the nitrogen cycle in the U.S. on radiative forcing. \*Biogeochemistry\*, 114\(1–3\), 25–40. https://doi.org/10.1007/s10533-012-9787-z](https://doi.org/10.1007/s10533-012-9787-z)
- Pui, D. Y. H., Chen, S. C., & Zuo, Z. (2014). PM2.5 in China: Measurements, sources, visibility and health effects, and mitigation. *Particuology*, 13(1), 1–26. <https://doi.org/10.1016/j.partic.2013.11.001>
- Seinfeld, J. H., & Pandis, S. N. (2016). *Atmospheric chemistry and physics: from air pollution to climate change*. John Wiley & Sons, Inc.
- Shephard, M. W., & Cady-Pereira, K. E. (2015). Cross-track Infrared Sounder (CrIS) satellite observations of tropospheric ammonia. *Atmos. Meas. Tech*, 8, 1323–1336. <https://doi.org/10.5194/amt-8-1323-2015>
- Shephard, M. W., Cady-Pereira, K. E., Luo, M., Henze, D. K., Pinder, R. W., Walker, J. T., Rinsland, C. P., Bash, J. O., Zhu, L., Payne, V. H., & Clarisse, L. (2011). TES ammonia retrieval strategy and global

observations of the spatial and seasonal variability of ammonia. *Atmospheric Chemistry and Physics*, 11(20), 10743–10763. <https://doi.org/10.5194/acp-11-10743-2011>

[Xu Zhenying, X., Liu, M., Song, Y., Wang, S., Xu, Z., Zhang, M., Zhang, L., Xu, T., Wang, T., Yan, C., Zhou, T., Sun, Y., Pan, Y., Hu, M., Zheng, M., & Zhu, T. \(2019\). High efficiency of livestock ammonia emission controls in alleviating particulate nitrate during a severe winter haze episode in northern China. Article in \*Atmospheric Chemistry and Physics\*, 19, 5605–5613. <https://doi.org/10.5194/acp-19-5605-2019>](#)

Yang, W., Ma, Q., Liu, Y., Ma, J., Chu, B., Wang, L., & He, H. (2018). Role of NH<sub>3</sub> in the Heterogeneous Formation of Secondary Inorganic Aerosols on Mineral Oxides. *Journal of Physical Chemistry A*, 122(30), 6311–6320. <https://doi.org/10.1021/acs.jpca.8b05130>

Zhu, L., Henze, D. K., Bash, J. O., Cady-Pereira, K. E., Shephard, M. W., Luo, M., & Capps, S. L. (2015). Sources and Impacts of Atmospheric NH<sub>3</sub>: Current Understanding and Frontiers for Modeling, Measurements, and Remote Sensing in North America. *Current Pollution Reports*, 1(2), 95–116. <https://doi.org/10.1007/s40726-015-0010-4>

Zhu, L., Henze, D. K., Cady-Pereira, K. E., Shephard, M. W., Luo, M., Pinder, R. W., Bash, J. O., & Jeong, G.-R. (2013). Constraining US ammonia emissions using TES remote sensing observations and the GEOS-Chem adjoint model. *Journal of Geophysical Research: Atmospheres*, 118(8), 3355–3368. <https://doi.org/10.1002/jgrd.50166>